

---

# CERTIFICATION FOR DIFFERENTIALLY PRIVATE PREDICTION IN GRADIENT-BASED TRAINING

---

PREPRINT

Matthew Wicker<sup>\*1,2</sup>, Philip Sosnin<sup>\*1</sup>, Igor Shilov<sup>1</sup>, Adrianna Janik<sup>3</sup>,  
Mark N. Müller<sup>4,5</sup>, Yves-Alexandre de Montjoye<sup>1</sup>, Adrian Weller<sup>2,6</sup>, Calvin Tsay<sup>1</sup>

<sup>1</sup>Department of Computing, Imperial College London, London, United Kingdom

<sup>2</sup>The Alan Turing Institute, London, United Kingdom

<sup>3</sup>Accenture Labs, Dublin, Ireland

<sup>4</sup>Department of Computer Science, ETH Zurich, Zurich, Switzerland

<sup>5</sup>LogicStar.ai, Zurich, Switzerland

<sup>6</sup>Department of Engineering, University of Cambridge, Cambridge, United Kingdom

## ABSTRACT

Differential privacy upper-bounds the information leakage of machine learning models, yet providing meaningful privacy guarantees has proven to be challenging in practice. The private prediction setting where model outputs are privatized is being investigated as an alternate way to provide formal guarantees at prediction time. Most current private prediction algorithms, however, rely on global sensitivity for noise calibration, which often results in large amounts of noise being added to the predictions. Data-specific noise calibration, such as smooth sensitivity, could significantly reduce the amount of noise added, but were so far infeasible to compute exactly for modern machine learning models. In this work we provide a novel and practical approach based on convex relaxation and bound propagation to compute a provable upper-bound for the local and smooth sensitivity of a prediction. This bound allows us to reduce the magnitude of noise added or improve privacy accounting in the private prediction setting. We validate our framework on datasets from financial services, medical image classification, and natural language processing and across models and find our approach to reduce the noise added by up to order of magnitude.

## 1 Introduction

Modern machine learning systems have shown significant potential impact across diverse domains such as medical imaging, autonomous driving, and sentiment analysis (Bommasani et al., 2021). These models are however trained on user data and have been shown to be prone to memorize (at least part of) their training data (Song et al., 2017; Carlini et al., 2023). In the EU, this could render the trained model personal data and make it subjected to GDPR (Gadotti et al., 2024), strongly limiting its applicability. Art 29 WP guidance indeed states that individual should not be able to be singled out for a model to be consider anonymous according to GDPR.

Differential privacy (DP) is providing formal guarantees of privacy protection. It is typically achieved for machine learning models through DP-SGD (Abadi et al., 2016) which privatizes model parameters, and by the post-processing theorem, any predictions released (Dwork et al., 2014). This approach to privacy can come with challenges

including increased sample complexity of private learning (Beimel et al., 2013) and reduced model utility (Alvim et al., 2012; Li et al., 2022; Sander et al., 2023).

Differentially private predictions has been studied as a means to potentially alleviate some of these issues (Dwork & Feldman, 2018). In the private prediction setting, the model itself has no privacy protections; rather, their predictions are privatized before release. These predictions can then be provided to users, e.g. in the increasingly popular machine-learning-as-a-service setup (Bommasani et al., 2021), or used for downstream tasks including differentially private model training. Originally proposed in 2016, PATE (Papernot et al., 2016) has recently been used in new applications such as in LLM in-context learning (Duan et al., 2024) and collaborative learning (Choquette-Choo et al., 2021)<sup>2</sup>.

---

<sup>2</sup>See Appendix A for a more in-depth discussion of related literature.

So far however, privatizing predictions has often outperformed by differentially private training. Previous work, including (van der Maaten & Hannun, 2020), hypothesized this to be due to private prediction suffering from “naïve” accounting and lack of specificity. Private predictions mechanisms indeed use a model’s global sensitivity, i.e., the worst-case sensitivity over all possible input datasets, for noise calibration. This is often not representative of risks associated with a given dataset and results in large amount of noise being added.

Traditional methods for data-specific noise calibration, such as smooth sensitivity (Nissim et al., 2007) could substantially improve accounting in the private prediction setting. Unfortunately, computation of smooth sensitivity for general machine learning models is intractable, as it requires analyzing non-convex model behavior across a large space of potential datasets.

In this work, we leverage advances in bound propagation to develop a novel convex relaxation of gradient-based training regimes (e.g., stochastic gradient descent and Adam). These allow us to provably bound the set of all reachable model parameters when  $k$  individuals are added or removed from the given dataset. Using this set of reachable parameters from adjacent datasets, we can then compute an upper-bound on the local sensitivity, and subsequently the smooth sensitivity, of a given prediction. We then use this upper-bound to substantially improve privacy-utility trade-off of a private prediction mechanism.

We show our approach to improve privacy accounting or reduce the additional noise by up to an order of magnitude across fully connected, convolutional, and large language models on datasets from financial services, medical image recognition, and natural language processing, in some cases leading to a more than 25% increase in accuracy. We additionally show that our bounds are able to bolster orthogonal developments in machine unlearning where we can compute even tighter bounds on a prediction’s sensitivity.

In summary this paper contributes the following:

- We provide a novel algorithm (developed concurrently with (Sosnin et al., 2024)) for bounding the reachable set of model parameters given a bound  $k$  on the number of individuals that can be added/removed from the dataset.
- We use our bound on reachable model parameters to bound both local sensitivity and smooth sensitivity in the differentially private prediction setting, and we prove necessary bounds to use the smooth sensitivity to reduce the amount of noise or tighten privacy accounting.
- We validate our bounds with extensive experiments on a variety of datasets from finance, medical imaging, and sentiment classification including fully connected, convolutional, and large language models. We find that our approach improves privacy accounting by nearly an order of magnitude.

## 2 Preliminaries

We denote a machine learning model as a parametric function  $f$  with parameters  $\theta \in \Theta$ , which maps from features  $x \in \mathbb{R}^n$  to labels  $y \in \mathcal{Y}$ . We consider supervised learning in the classification setting with a labeled dataset  $\mathcal{D} = \{(x^{(i)}, y^{(i)})\}_{i=1}^N$ . The model parameters are trained, starting from some initialization  $\theta'$ , using a gradient-based algorithm, denoted as  $M$ , as  $\theta = M(f, \theta', \mathcal{D})$ . In other words, given a model, initialization, and dataset, the training function  $M$  returns the “trained” parameters  $\theta$ . The function  $M$  is typically taken to be stochastic with randomness stemming from the initialization, batch ordering, and any noise added. For such a function,  $\epsilon$ -differential privacy is defined as:

**Definition 1.  $\epsilon$ -Differential Privacy (Dwork et al., 2014)** Given a learning algorithm  $M(\cdot)$ , we say it is  $\epsilon$ -differentially private if,  $\forall S \subset \Theta$  and for all pairs of datasets  $\mathcal{D}, \mathcal{D}'$  which only differ in one element:

$$\mathbb{P}(M(f, \theta', \mathcal{D}) \in S) \leq e^\epsilon \mathbb{P}(M(f, \theta', \mathcal{D}') \in S) \quad (1)$$

which intuitively means that the addition or removal of a single data point has a probabilistically limited effect on the outcome of the learning algorithm.

In this work, we focus on differential privacy on the level of predictions, formally:

**Definition 2.  $\epsilon$ -Differentially Private Predictions (Dwork & Feldman, 2018)** Let  $R$  be an algorithm that, given a dataset  $\mathcal{D} \in (X \times Y)^N$  and a point  $x$ , produces a value in  $Y$ . We say that  $R$  is an  $\epsilon$ -differentially private algorithm if for every  $x \in X$ , the output  $R(f, \theta', \mathcal{D}, x)$  is  $\epsilon$ -differentially private with respect to  $\mathcal{D}$ . We use  $R(f, \theta', \mathcal{D}, \cdot)$  as an abbreviation of the full function:  $R = f^{M(f, \theta', \mathcal{D})}(x)$ , where learning algorithm  $M$  returns a parameter given  $\mathcal{D}$  and  $\theta'$ .

## 3 Methodology and Computations

In this section, we begin by introducing formal definitions of local sensitivity and privacy-safe certification. We then detail how bounding these notions can reduce the noise added in private prediction settings (§ 3.1.1) and improve privacy accounting in private prediction (§ 3.1.2). We also discuss how these results could enhance current machine unlearning methods (§ 3.1.3). We then show how, for a parameterized machine learning model, these definitions can be reasoned about (i.e., formally proven) through the notion of valid parameter-space bounds on the output of a learning algorithm. We then present an algorithmic framework for efficiently computing parameter-space bounds that enable practical certification of our properties.

Before describing our approach to data-dependent differentially private predictions, we establish the baseline setting based on global sensitivity. We consider a machine learning model that releases predictions in a no-box setting, i.e., we take the output of the model,  $f^{M(f, \mathcal{D}, \theta')}(x)$ , to be a

binary label of the model’s prediction. To privatize the response one releases predictions according to

$$R(x) := \begin{cases} 1 & \text{if } f^{M(f, \mathcal{D}, \theta')}(x) + \text{Lap}(1/\epsilon) > 0.5 \\ 0 & \text{otherwise} \end{cases} \quad (2)$$

which satisfies Definition 1. This can be interpreted as releasing a label in PATE but with a single teacher model and therefore only one vote (Papernot et al., 2016). While the above applies to binary classification, it can be generalized to multi-class or bounded regression problems as detailed in Papernot et al. (2016).

### 3.1 Privacy Safe Certification

To simplify our exposition, we consider the privacy setting by defining the set of all datasets with  $k$  or fewer elements added or removed from  $\mathcal{D}$  as  $\mathcal{T}_k^p(\mathcal{D})$ . We now define the local sensitivity of a prediction under any  $k$  or fewer additions/removals:

**Definition 3. (Local Sensitivity)** *The local sensitivity of a prediction made by a machine learning model  $f$  trained by  $M$  at a point  $x$ , i.e.,  $y = f^{M(f, \theta', \mathcal{D})}(x)$ , is defined as:*

$$\max_{\mathcal{D}' \in \mathcal{T}_k^p(\mathcal{D})} |f^{M(f, \theta', \mathcal{D}')} (x) - f^{M(f, \theta', \mathcal{D})}(x)| \quad (3)$$

We will define the solution to the above problem with the notation  $\Delta_{\mathcal{D}}^k f|_x$  where  $k$  is the same as in the definition of  $\mathcal{T}_k^p$ .

In this work we also define the notion of a privacy-safe prediction. Intuitively, a prediction is privacy-safe if every possible model resulting from the addition and/or removal of  $k$  points gives the same prediction.

**Definition 4. (Privacy-Safety)** *A prediction at a point  $x$  made by a machine learning model  $f$  trained by  $M$ , i.e.,  $y = f^{M(f, \theta', \mathcal{D})}(x)$ , is said to be a privacy-safe prediction if:*<sup>3</sup>

$$\Delta_{\mathcal{D}}^k f|_x = 0 \quad (4)$$

Unfortunately, for general machine learning models exactly computing  $\Delta_{\mathcal{D}}^k f|_x$  is practically infeasible. As adversarial robustness is NP-complete (Katz et al., 2017), exactly computing Delta does not admit a polynomial time solution. Instead, we are interested in *certifying* the local sensitivity of a prediction which consists of computing an upper-bound, LS such that we can soundly prove that:  $\Delta_{\mathcal{D}}^k f|_x \leq \text{LS}(\mathcal{T}_k^p, x)$ . Computation of this bound will be the subject of Sections 3.2 and 3.3. In the next sections, we will discuss uses of  $\Delta_{\mathcal{D}}^k f|_x$ .

#### 3.1.1 Noise Reduction with Privacy-Safe Certification

As described at the beginning of this section, the private prediction mechanism  $f^{M(f, \mathcal{D}, \theta')}(x) + \text{Lap}(1/\epsilon)$  satisfies Definition 2 with the global sensitivity of  $f^\theta$  being 1. Unfortunately, adding noise  $\sim \text{Lap}(1/\epsilon)$  typically comes with

<sup>3</sup>Requiring strict equality restricts us to classification or quantized regression; this may be relaxed in future works.

a significant decrease in model utility for small  $\epsilon$ . To reduce this noise, we use  $\Delta_{\mathcal{D}}^k f|_x$  to compute the  $\beta$  smooth sensitivity:

**Theorem 3.1. (Smooth Sensitivity, Nissim et al. (2007))** *The  $\beta$ -smooth sensitivity of the prediction response function  $R$  is upper-bounded by:*

$$S_{\mathcal{D}}^\beta(x) = \max_{k \in \mathbb{N}^+} \Delta_{\mathcal{D}}^k f|_x \exp(-2\beta k) \quad (5)$$

In practice, it may seem like Theorem 3.1 requires us to compute an infinite set of sensitivities (for various  $k$ ), however, in quantized-output settings, the decreasing nature of the exponential ensures we only have to compute finitely many. This is further discussed in Appendix C. Given Theorem 3.1 and taking directly from Nissim et al. (2007), we have that:

1. If  $\beta < \frac{\epsilon}{2(g+1)}$  and  $g > 1$  the algorithm that returns  $f^M(x) + \frac{2(g+1)S_{\mathcal{D}}^\beta(x)}{\epsilon} \cdot \eta$  where  $\eta$  is a random variable distributed according to the density  $\frac{1}{1+|z|^g}$ , is  $\epsilon$  differentially private<sup>4</sup>.
2. If  $\beta \leq \frac{\epsilon}{2 \ln(2/\delta)}$  and  $\delta \in (0, 1)$  the algorithm that returns  $f^M(x) + \frac{2S_{\mathcal{D}}^\beta(x)}{\epsilon} \cdot \eta$  where  $\eta \sim \text{Lap}(1)$ , is  $(\epsilon, \delta)$  differentially private.

Both of the above allow us to directly scale the noise added to the machine learning models prediction by the local smooth sensitivity (proportional to  $\Delta_{\mathcal{D}}^k f|_x$ ) rather than the global sensitivity.

#### 3.1.2 Privacy Accounting with Privacy-Safe Certification

We now assume that we keep the noise scaling proportional to the global sensitivity of the function and instead use our bound on the smooth sensitivity of our function to perform better privacy accounting. In particular, assuming one returns the prediction according to the global sensitivity, we can use the smooth sensitivity to do tighter privacy accounting. We have the following theorem, which we prove in Appendix D.1:

**Theorem 3.2. (Tighter Privacy Accounting)** *Releasing a prediction at a point  $x$  according to  $f^\theta(x) + \text{Lap}(1/\epsilon)$ , satisfies  $(\epsilon^S, \delta)$  differential privacy with  $\delta \in (0, 1)$  and*

$$\epsilon^S = \frac{\ln(2/\delta)}{k^*} W_0 \left( \frac{2\epsilon k^*}{\ln(2/\delta)} \right), \quad (6)$$

where  $W_0$  is the Lambert  $W$  function and  $k^* = \arg \max_{k \in \mathbb{N}^+} \Delta_{\mathcal{D}}^k f|_x \exp(-2\beta k)$  for  $\beta = \epsilon^S / (2 \ln(2/\delta))$ .

<sup>4</sup>We take  $g = 2$ , giving  $\eta \sim \text{Cauchy}(1)$ .

---

**Algorithm 1: ABSTRACT GRADIENT TRAINING FOR PRIVACY AND UNLEARNING**


---

**input :**  $f$  - ML model,  $\theta'$  - param. initialisation,  $\mathcal{D}$  - nominal dataset,  $E$  - epochs,  $\alpha$  - learning rate,  $\mathcal{T}_k^*$  - allowable dataset perturbations,  $\gamma$  - optional clipping parameter.  
**output:**  $\theta$  - nominal SGD parameter,  $[\theta_L, \theta_U]$  - reachable parameter interval.

```

1  $\theta \leftarrow \theta'; [\theta_L, \theta_U] \leftarrow [\theta', \theta']$  // Initialise nominal parameter and interval bounds.
2 for  $E$ -many epochs do
3   for each batch  $\mathcal{B} \subset \mathcal{D}$  do
4     /* Compute the nominal SGD parameter update. */
4      $\Delta\theta \leftarrow \frac{1}{|\mathcal{B}|} \sum_{(x,y) \in \mathcal{B}} \text{Clip}_\gamma [\nabla_{\theta} \mathcal{L}(f^\theta(x), y)]$  // Compute descent direction.
5      $\theta \leftarrow \theta - \alpha \Delta\theta$  // Update the nominal parameter.
6     /* Bound on the nominal parameters under  $k$  removals and/or additions. */
6      $\Delta\Theta \leftarrow \left\{ \frac{1}{|\tilde{\mathcal{B}}|} \sum_{(\tilde{x}, \tilde{y}) \in \tilde{\mathcal{B}}} \text{Clip}_\gamma [\nabla_{\theta'} \mathcal{L}(f^{\theta'}(\tilde{x}), \tilde{y})] \mid \tilde{\mathcal{B}} \in \mathcal{T}_k^*(\mathcal{B}), \theta' \in [\theta_L, \theta_U] \right\}$  // Define the set of all descent directions.
7     Compute  $\Delta\theta_L, \Delta\theta_U$  s.t.  $\Delta\theta_L \preceq \Delta\theta \preceq \Delta\theta_U \quad \forall \Delta\theta \in \Delta\Theta$  // Compute lower and upper bounds on the descent direction.
8      $\theta_L \leftarrow \theta_L - \alpha \Delta\theta_U; \quad \theta_U \leftarrow \theta_U - \alpha \Delta\theta_L$  // Update the reachable parameter interval.
9 return  $\theta, [\theta_L, \theta_U]$ 
    
```

---

### 3.1.3 Provable Unlearning with Safe Certification

While our focus is on privacy, we note here that our results can be relevant to the machine unlearning literature. In the case of unlearning, we first denote the set of all datasets with  $k$  or fewer elements removed as  $\mathcal{T}_k^u(\mathcal{D})$ . Then, replacing  $\mathcal{T}_k^p(\mathcal{D})$  by  $\mathcal{T}_k^u(\mathcal{D})$  in the previous sections, one can compute bounds on the sensitivity under the removal of data points, and corresponding ‘‘unlearning-safe’’ certificates. We explore this setting in more detail in Appendix E.

The bounds on the sensitivity may be considerably tighter than the privacy case, due to the fact that  $|\mathcal{T}_k^u| < |\mathcal{T}_k^p|$ . Moreover, satisfying Definition 4 for unlearning can enhance state-of-the-art retraining approaches for unlearning, e.g., SISA (Bourtoule et al., 2021). Upon receiving an unlearning request, these methods must take the affected model in the ensemble offline to undergo partial retraining. Adversaries may therefore perform a denial-of-service attack by simultaneously submitting  $\mathcal{O}(d \log(d))$  unlearning requests, at which point the entire ensemble is expected to be offline for retraining, provided the ensemble comprises  $d$  or fewer models. Given our approach, despite each model receiving up to  $k$  simultaneous unlearning requests, we may still issue predictions proven to be unlearning-safe, thus increasing the required number of unlearning requests to achieve denial-of-service to  $\mathcal{O}(kd \log(kd))$ -many simultaneous requests.

### 3.2 Valid Parameter Space Bounds

In this section, we lay the foundations of our framework by defining valid *parameter space bounds* as an intermediate step toward upper-bounding Definition 3 and 4. We

start by introducing two assumptions. First, for expositional purposes, we assume that bounds take the form of an interval:  $[\theta_L, \theta_U]$  s.t.  $\forall i, [\theta_L]_i \leq [\theta_U]_i$ . This can be relaxed to linear constraints for more expressive parameter bounds. Second, we assume that the parameter initialization  $\theta'$  and data ordering are both arbitrary, but fixed. The latter assumption on data ordering is purely an expositional convenience that is relaxed in Appendix D.

**Definition 5. (Valid Parameter-Space Bounds)** A domain  $T$  defined by bounds  $[\theta_L, \theta_U]$  is said to be a valid parameter-space bound if and only if:

$$\forall \mathcal{D}' \in \mathcal{T}_k^*(\mathcal{D}), \quad M(f, \theta', \mathcal{D}') \in T \quad (7)$$

where  $\star \in \{p, u\}$  controls if we are in the privacy or unlearning settings, respectively.

Using this definition we can shift the certification of privacy/unlearning-safe predictions (Definition 4) from relying on computations over the set of all perturbed datasets to being over an (over-approximated) parameter-space domain  $T$ . In particular we have:

**Lemma 1.** For any valid parameter-space bounds  $T$  satisfying Definition 5, proving that  $\forall \theta \in T, |f^\theta(x) - f^{M(f, \theta', \mathcal{D})}(x)| \leq \rho$  suffices as proof that  $\Delta_{\mathcal{D}}^k f|_x \leq \rho$ , and therefore bound propagation w.r.t.  $T$  satisfies as an upper-bound to Definition 3 and where  $\rho = 0$  as proof of Definition 4.

While it is infeasible to work in the space of all perturbed datasets  $\mathcal{T}_k^*$ , Lemma 1 defines corresponding properties that can be computed/bounded straightforwardly starting with a closed parameter set  $T$ . Certifying for any given  $x$  that  $f^\theta(x)$  is constant for any  $\theta \in T$  is discussed in more detail in Section 3.4.

### 3.3 Abstract Gradient Training

This section presents the core of our framework: an algorithm that can compute valid parameter space bounds. We call this algorithm *Abstract Gradient Training* (AGT) and present it in Algorithm 1.

Algorithm 1 proceeds by soundly bounding effect of the worst-case removals and/or additions for each batch encountered during training. We therefore have the following theorem, which is proved in Appendix D:

**Theorem 3.3.** *Given a model  $f$ , dataset  $D$ , arbitrary but fixed initialization,  $\theta'$ , bound on the number of added removed individuals,  $k$ , and learning hyper-parameters including: batch size  $b$ , number of epochs  $E$ , and learning rate  $\alpha$ , Algorithm 1 returns valid parameter-space bounds on the stochastic gradient training algorithm,  $M$ , that satisfy Definition 5.*

We note that the clipping procedure  $\text{Clip}_\gamma$  in Algorithm 1 is a truncation operator that clamps all elements of its input to be between  $-\gamma$  and  $\gamma$ , while leaving those within the range unchanged. This is distinct from the  $\ell_2$ -norm clipping typically employed by privacy-preserving mechanisms such as DP-SGD (Abadi et al., 2016). In this work, we chose to use the truncation operator as it is more amenable to bound-propagation.

The set  $\Delta\theta = \{\cdot \mid \tilde{\mathcal{B}} \in \mathcal{T}_k^*(\mathcal{B}), \theta' \in [\theta_L, \theta_U]\}$  (line 6 of Algorithm 1) represents the set of all possible descent directions that can be reached at this iteration under the given dataset perturbations. In particular,  $\theta'$  accounts for any  $k$  removals from and/or additions to each *previously seen* batch (via valid parameter-space bounds), while  $\tilde{\mathcal{B}}$  represents the effect of  $k$  removals/additions from the *current* batch. Computing this set exactly is not tractable, so we instead compute an element-wise, over-approximated, lower and upper bound  $\Delta\theta_L, \Delta\theta_U$  using the procedure in Theorem 3.4. These bounds are then combined with  $\theta_L, \theta_U$  using sound interval arithmetic to produce a new valid parameter-space bound.

**Theorem 3.4** (Bounding the descent direction). *Given a nominal batch  $\mathcal{B} = \{(x^{(i)}, y^{(i)})\}_{i=1}^b$  with batchsize  $b$ , a parameter set  $[\theta_L, \theta_U]$  and clipping level  $\gamma$ , the parameter update*

$$\Delta\theta = \frac{1}{|\tilde{\mathcal{B}}|} \sum_{(\tilde{x}^{(i)}, \tilde{y}^{(i)}) \in \tilde{\mathcal{B}}} \text{Clip}_\gamma \left[ \nabla_{\theta'} \mathcal{L} \left( f^{\theta'}(\tilde{x}^{(i)}), \tilde{y}^{(i)} \right) \right]$$

is bounded element-wise by

$$\Delta\theta_L = \frac{1}{b - k_r + k_a} \left( \text{SEMin}_{b-k_r} \left\{ \delta_L^{(i)} \right\}_{i=1}^b - k_a \gamma \mathbf{1}_d \right)$$

$$\Delta\theta_U = \frac{1}{b - k_r + k_a} \left( \text{SEMax}_{b-k_r} \left\{ \delta_U^{(i)} \right\}_{i=1}^b + k_a \gamma \mathbf{1}_d \right)$$

for any perturbed batch  $\tilde{\mathcal{B}}$  derived from  $\mathcal{B}$  by adding up to  $k_a$  and removing up to  $k_r$  data-points. The terms  $\delta_L^{(i)}, \delta_U^{(i)}$  are sound bounds that account for the worst-case effect of

additions/removals in any previous iterations. That is, they bound the gradient given any parameter  $\theta^* \in [\theta_L, \theta_U]$  in the reachable set, i.e.  $\delta_L^{(i)} \preceq \delta^{(i)} \preceq \delta_U^{(i)}$  for all

$$\delta^{(i)} \in \left\{ \text{Clip}_\gamma \left[ \nabla_{\theta'} \mathcal{L} \left( f^{\theta'}(x^{(i)}), y^{(i)} \right) \right] \mid \theta' \in [\theta_L, \theta_U] \right\}.$$

The operations  $\text{SEMax}_a$  and  $\text{SEMin}_a$  correspond to taking the sum of the element-wise top/bottom- $a$  elements. For  $\mathcal{T}_k^p(\mathcal{D})$  we use  $k_a = k_r = k$ . We also note that in the unlearning setting  $\mathcal{T}_k^u(\mathcal{D})$  can be recovered by defining  $k_a = 0, k_r = k$  in Theorem 3.4.

**Computing Gradient Bounds.** Many of the computations in Algorithm 1 are typical computations performed during stochastic gradient descent. However, lines 6-7 involve bounding non-convex optimization problems. In particular, bounding the descent directions using Theorem 3.4 requires bounds  $\delta_L^{(i)}, \delta_U^{(i)}$  on the gradients of a machine learning model  $f(x, \theta)$  w.r.t. perturbations about  $\theta$ . We note that solving problems of the form  $\min \{\cdot \mid x \in [x_L, x_U]\}$  has been well-studied in the context of adversarial robustness certification (Huchette et al., 2023). However, optimizing over both the input and the parameters (as is required to bound the gradients), e.g.,  $\min \{\cdot \mid x \in [x_L, x_U], \theta \in [\theta_L, \theta_U]\}$ , is relatively less studied, and to-date has appeared primarily in certification of probabilistic neural networks (Wicker et al., 2020; Singh et al., 2019). In the remainder of this paper, we focus our attention on classical neural networks, where an explicit Interval Bound Propagation (IBP) (Gowal et al., 2018) approach can be employed to bound the required optimization problems. Details of computing gradient bounds for neural network models using IBP can be found in Appendix B. This approach can also be generalized to cover non-neural network machine learning models.

### 3.4 Algorithm Analysis and Discussion

#### Computing Privacy and Unlearning Safe Certificates.

Lemma 1 establishes that once we have our parameter bounds (i.e., from Algorithm 1) we can bound  $\Delta_{\mathcal{D}}^k f|_x$  and potentially compute a certificate. This is done by propagating the input  $x$  through the neural network with the interval from Algorithm 1 as the networks parameters (as in e.g., Wicker et al. (2020)) which results in an interval over output space. It is then straight-forward to compute the largest distance between elements of this output interval, or in the case of classification the largest change in the prediction e.g., if the prediction changes (Gowal et al., 2018). Following Lemma 1, these computations could then be taken as the function  $\text{LS}(\mathcal{T}_k^*, x)$  which upper-bounds  $\Delta_{\mathcal{D}}^k f|_x$  and can be used in each of our tighter privacy analysis bounds.

#### Computing Bounds on the Smooth Sensitivity.

Given bounds on the local sensitivity via our privacy-safe certificates, we now turn to bounding the smooth sensitivity  $S_{\mathcal{D}}^\beta(x)$ . We first note that  $S_{\mathcal{D}}^\beta(x) = \max_k \Delta_{\mathcal{D}}^k f|_x \exp(-2\beta k) \leq \max_k \text{LS}(\mathcal{T}_k^*, x) \exp(-2\beta k)$ . Since  $\text{LS}(\mathcal{T}_k^*, x) \in \{0, 1\}$

(for binary classification) and is non-decreasing in  $k$ , bounding  $S_{\mathcal{D}}^{\beta}(x)$  amounts to finding the smallest  $k$  for which we *cannot* provide a certificate of privacy safety. Labelling this critical value  $k^*$ , the smooth sensitivity  $S_{\mathcal{D}}^{\beta}(x)$  is bounded by  $\exp(-2\beta k^*)$ . While the tightest upper bound on  $S_{\mathcal{D}}^{\beta}(x)$  is achieved at  $k^*$ , looser (but still sound) upper bounds are given by  $\exp(-2\beta k)$  for any  $k < k^*$ . Therefore, computing the exact  $k^*$  is not required and computing looser bounds comes with a corresponding trade-off between computational complexity and tightness. In many cases, only a handful of values of  $k$  are required to capture most of the privacy benefits, requiring only a small number of runs of Algorithm 1. Details of computing bounds on the smooth sensitivity is described in more detail in Appendix C.

**Computational Complexity.** To analyze the time complexity of our algorithm in comparison to standard stochastic gradient descent (SGD), we focus on the operations described in Theorem 3.4. First, computing the gradient bounds  $\delta_L^{(i)}$  and  $\delta_U^{(i)}$  for each sample  $i$  in the batch using interval propagation requires at most four times the cost of regular training (see Appendix B). Once the bounds are computed, selecting the top or bottom  $k$  gradient bounds has a time complexity of  $\mathcal{O}(b)$ , where  $b$  is the batch size. Thus, the time complexity for a single run of Algorithm 1 is a constant factor times the complexity of standard training.

Empirically, we observe that a single run of AGT incurs a wall-clock time that is 2 to 4 times that of regular training. Although improved privacy guarantees can be obtained using just one value of  $k$ , running Algorithm 1 for multiple values  $k \in \{k_1, \dots, k_M\}$  provides tighter guarantees. In practice, fewer than  $M = 10$  runs of Algorithm 1 are generally sufficient to achieve most of the privacy benefits, which we explore further in Appendix C. At inference time, the largest value of  $k \in \{k_1, \dots, k_M\}$  for which privacy-safe certificates can be provided must be determined (e.g., via binary search). This incurs a cost of approximately  $4 \log M$  times the cost of standard inference.

## 4 Experiments

In this section we provide experimental validation of our approach to certification of privacy-safe predictions. We provide further hyper-parameter details in Appendix F. and provide a code repository to reproduce our experiments at: <https://github.com/psosnin/AbstractGradientTraining> All experiments are run on a server with 2x AMD EPYC 9334 CPUs and 2x NVIDIA L40 GPUs. For each task, we present analogous results for unlearning certification in Appendix F.

### 4.1 Blobs Dataset

In Figure 1, we consider a dataset of 3000 total samples from two distinct isotropic Gaussian distributions with the goal of predicting the distribution origin of each sample in a supervised learning task.. We train a single-layer neural

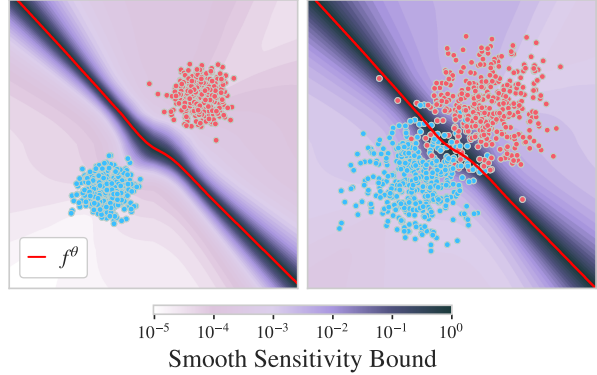


Figure 1: We use the “blobs” dataset to visualize the smooth sensitivity bounds given by AGT for  $(\epsilon, \delta) = (1.0, 10^{-5})$ . The red line is the decision boundary given by the nominal parameter  $\theta$ .

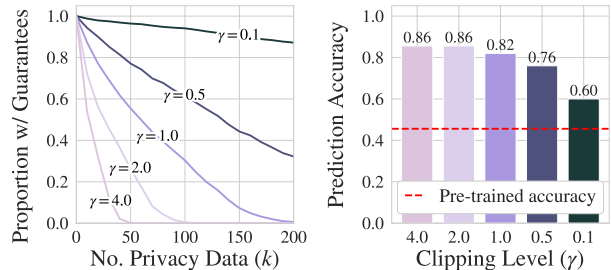


Figure 2: Performance on new diseased class in OCT-MNIST Fine-Tuning ( $b = 5000$ ). Left: Proportion of the test set with privacy-safe predictions. Right: Prediction accuracy on the Drusen class.

network with 512 hidden neurons using AGT and visualize the resulting smooth sensitivity bounds. These bounds are computed for the  $(\epsilon, \delta)$ -DP mechanism outlined in Section 3.1.1, with  $\beta = \epsilon/(2 \ln(2/\delta))$ . Near the decision boundary, the smooth sensitivity bounds are close to the global sensitivity of 1. However, our upper bound decays exponentially as the distance from the decision boundary increases, providing significantly tighter privacy guarantees for the majority of predictions on the test data.

In cases where the data is perfectly separable, AGT yields stronger privacy guarantees. On the other hand, where the blobs overlap, the influence of adding or removing  $k$  points becomes more significant, leading to looser bounds from AGT. In Figure 5a, we highlight that AGT allows for privacy guarantees that are orders of magnitude tighter than the naive approach, either preserving high accuracy with much lower privacy loss or producing stronger  $(\epsilon^S, \delta)$ -DP guarantees.

### 4.2 MedMNIST Image Classification

Next, we consider a real-world, privacy-critical dataset with larger scale inputs: classification of medical images

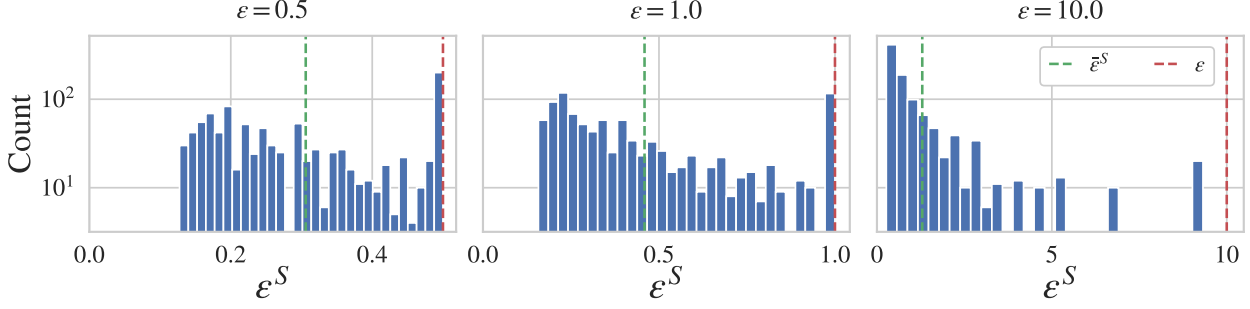


Figure 3: Distribution of tightened  $\epsilon^S$  guarantees on the OCT-MNIST test data obtained via AGT for  $\delta = 10^{-5}$  and various global  $\epsilon$ . The mean  $\epsilon^S$  and global  $\epsilon$  are shown in green and red, respectively.

from the retinal OCT (OCT-MNIST) dataset of MEDMNIST (Yang et al., 2021). We consider a binary classification over this dataset, where a model is tasked with predicting whether an image is normal or abnormal (the latter combines three distinct abnormal classes from the original dataset). The model comprises two convolutional layers of 16 and 32 filters and an ensuing 100-node dense layer, corresponding to the ‘small’ architecture from Goyal et al. (2018). To demonstrate our framework, we consider a base model trained on public data and then fine-tuned on new, privacy-sensitive data, corresponding to the 7754 Drusen samples (a class of abnormality omitted from initial training). First, we train the complete model excluding this using standard stochastic gradient descent. We then fine-tune only the dense layer weights to recognise the new class, with a mix of 50% Drusen samples per batch.

Figure 2 shows the proportion of predictions for the Drusen samples that are covered with privacy-safe certificates, as well as the nominal accuracies. The accuracy on the Drusen data ranges from approximately 0.6 up to 0.86 after fine-tuning. The final utility is highly dependent on the value of the clipping level  $\gamma$ . Decreasing the value of  $\gamma$  reduces the accuracy of the model, but increases the proportion of points for which we can provide certificates of privacy safety. For small values of  $k$ , our framework is able to provide certificates of privacy safety for well over 90% of test-set inputs.

Figure 5b shows the corresponding usage of our privacy-safe certificates for computing tighter privacy guarantees (for the model with  $\gamma = 1.0$ ). As above, we use our privacy-safe certificates to compute a bound on the smooth sensitivity for each prediction on the test data set. When using the global sensitivity, the model utility falls rapidly towards 50% as the privacy loss  $\epsilon$  decreases. On the other hand, adding noise calibrated to our smooth sensitivity bounds (i.e.  $\sim \text{Cauchy}(6S_D^\beta(x)/\epsilon)$ ), maintains high accuracy for values of  $\epsilon$  up to 10x smaller than those afforded by the global sensitivity.

Figure 3 shows the distribution of tightened  $(\epsilon^S, \delta)$ -DP guarantees obtained from Theorem 3.2. We can see that the majority of points enjoy much tighter privacy guarantees when compared with the global sensitivity. However, we

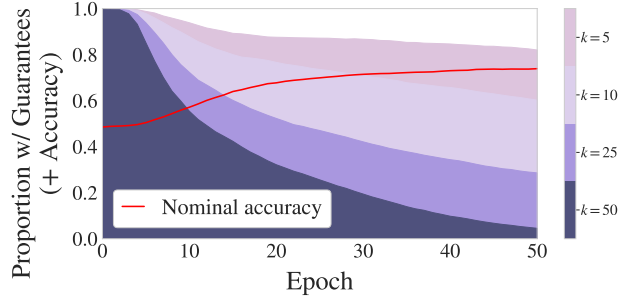


Figure 4: Proportion of test set queries with privacy-safe guarantees for the GPT-2 sentiment classification task at each training epoch ( $\gamma = 0.1$ ).

note that the global sensitivity gives pure  $\epsilon$ -DP guarantees, while our tightened guarantees hold for approximate ( $\delta > 0$ ) DP.

### 4.3 Generative Pre-Trained Transformers (GPT-2)

Finally, we consider fine-tuning GPT-2 (Radford et al., 2019) for sentiment analysis on the large-scale IMDb movie review dataset (Maas et al., 2011). In this setup, we assume that GPT-2 was pre-trained on publicly available data, distinct from the data used for fine-tuning, which implies no privacy risk from the pre-trained embeddings themselves. Under this assumption, we begin by encoding each movie review into a 768-dimensional vector using GPT-2’s embeddings.

We then train a fully connected neural network consisting of  $1 \times 100$  nodes, to perform binary sentiment classification (positive vs negative reviews). Figure 4 shows how the nominal accuracy and the proportion of certified data points evolve over the course of training. Although the initial accuracy is equivalent to random chance, fine-tuning allows us to reach an accuracy close to 0.80, while simultaneously preserving strong privacy guarantees using AGT. Each training run of the sentiment classification model with AGT takes approximately 55 seconds, compared to 25 seconds when using standard, un-certified, training in pytorch.



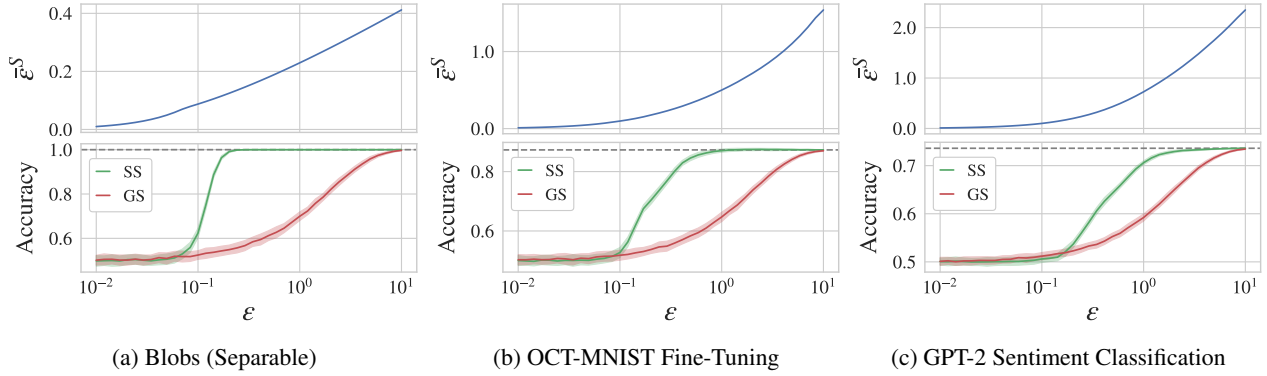


Figure 5: Usage of smooth sensitivity bounds for improving privacy guarantees and model utility. Top: Improvement in privacy guarantees from  $(\epsilon, 0)$  to  $(\epsilon^S, \delta)$  when using smooth sensitivity bounds. We plot the mean  $\epsilon^S$  for  $\delta = 10^{-5}$ . Bottom: Improvement in model utility when using smooth sensitivity bounds (SS) vs global sensitivity (GS).

In our experiments we find that we can certify points in the test data for values of  $k$  up to 50 (Figure 4). We note that our guarantees weaken with increased training time, indicating that stronger privacy guarantees can be obtained by terminating training early. Figure 5c shows the improvement in model utility or privacy guarantees when using our smooth sensitivity bounds. We can see that high accuracy is maintained for smaller values of  $\epsilon$  when compared with the global sensitivity approach.

## 5 Conclusion

In this work we introduce a framework for computing local (i.e., specific to a given prediction) certificates of  $\epsilon = 0$  privacy and unlearning. We provide a concrete implementation of this framework based on convex relaxations and bounds propagation that is able to provide these certificates to a significant proportion of users across real-world, privacy-critical applications including financial services, medical imaging, and natural language processing. In the future, we hope this framework enables stronger (but local) privacy guarantees that engender user trust and provides an important source of concrete privacy information toward the development of future privacy preserving techniques.

## References

- Abadi, M., Chu, A., Goodfellow, I., McMahan, H. B., Mironov, I., Talwar, K., and Zhang, L. Deep learning with differential privacy. In *Proceedings of the 2016 ACM SIGSAC conference on computer and communications security*, pp. 308–318, 2016.
- Alvim, M. S., Andrés, M. E., Chatzikokolakis, K., Degano, P., and Palamidessi, C. Differential privacy: on the trade-off between utility and information leakage. In *Formal Aspects of Security and Trust: 8th International Workshop, FAST 2011, Leuven, Belgium, September 12-14, 2011. Revised Selected Papers 8*, pp. 39–54. Springer, 2012.
- Bassily, R., Thakkar, O., and Guha Thakurta, A. Model-agnostic private learning. *Advances in Neural Information Processing Systems*, 31, 2018.
- Beimel, A., Nissim, K., and Stemmer, U. Characterizing the sample complexity of private learners. In *Proceedings of the 4th conference on Innovations in Theoretical Computer Science*, pp. 97–110, 2013.
- Bommasani, R., Hudson, D. A., Adeli, E., Altman, R., Arora, S., von Arx, S., Bernstein, M. S., Bohg, J., Bosselut, A., Brunskill, E., et al. On the opportunities and risks of foundation models. *arXiv preprint arXiv:2108.07258*, 2021.
- Bourtoule, L., Chandrasekaran, V., Choquette-Choo, C. A., Jia, H., Travers, A., Zhang, B., Lie, D., and Papernot, N. Machine unlearning. In *2021 IEEE Symposium on Security and Privacy (SP)*, pp. 141–159. IEEE, 2021.
- Carlini, N., Chien, S., Nasr, M., Song, S., Terzis, A., and Tramer, F. Membership inference attacks from first principles. In *2022 IEEE Symposium on Security and Privacy (SP)*, pp. 1897–1914. IEEE, 2022.
- Carlini, N., Ippolito, D., Jagielski, M., Lee, K., Tramer, F., and Zhang, C. Quantifying memorization across neural language models. In *The Eleventh International Conference on Learning Representations*, 2023.
- Choquette-Choo, C. A., Dullerud, N., Dziedzic, A., Zhang, Y., Jha, S., Papernot, N., and Wang, X. Capc learning: Confidential and private collaborative learning. In *International Conference on Learning Representations*, 2021.
- Duan, H., Dziedzic, A., Papernot, N., and Boenisch, F. Flocks of stochastic parrots: Differentially private prompt learning for large language models. *Advances in Neural Information Processing Systems*, 36, 2024.
- Dwork, C. and Feldman, V. Privacy-preserving prediction. In *Conference On Learning Theory*, pp. 1693–1702. PMLR, 2018.



- Dwork, C., Roth, A., et al. The algorithmic foundations of differential privacy. *Foundations and Trends® in Theoretical Computer Science*, 9(3–4):211–407, 2014.
- Gadotti, A., Rocher, L., Houssiau, F., Crețu, A.-M., and de Montjoye, Y.-A. Anonymization: The imperfect science of using data while preserving privacy. *Science Advances*, 10(29):eadn7053, 2024.
- Gehr, T., Mirman, M., Drachler-Cohen, D., Tsankov, P., Chaudhuri, S., and Vechev, M. Ai2: Safety and robustness certification of neural networks with abstract interpretation. In *2018 IEEE symposium on security and privacy (SP)*, pp. 3–18. IEEE, 2018.
- Gowal, S., Dvijotham, K., Stanforth, R., Bunel, R., Qin, C., Uesato, J., Arandjelovic, R., Mann, T., and Kohli, P. On the effectiveness of interval bound propagation for training verifiably robust models. *arXiv preprint arXiv:1810.12715*, 2018.
- Guo, C., Goldstein, T., Hannun, A., and Van Der Maaten, L. Certified data removal from machine learning models. *arXiv preprint arXiv:1911.03030*, 2019.
- Huang, Y. and Canonne, C. L. Tight bounds for machine unlearning via differential privacy. *arXiv preprint arXiv:2309.00886*, 2023.
- Huchette, J., Muñoz, G., Serra, T., and Tsay, C. When deep learning meets polyhedral theory: A survey. *arXiv preprint arXiv:2305.00241*, 2023.
- Katz, G., Barrett, C., Dill, D. L., Julian, K., and Kochenderfer, M. J. Reluplex: An efficient smt solver for verifying deep neural networks. In *Computer Aided Verification: 29th International Conference, CAV 2017, Heidelberg, Germany, July 24–28, 2017, Proceedings, Part I 30*, pp. 97–117. Springer, 2017.
- Li, X., Tramer, F., Liang, P., and Hashimoto, T. Large language models can be strong differentially private learners. In *International Conference on Learning Representations*, 2022.
- Ligett, K., Neel, S., Roth, A., Waggoner, B., and Wu, S. Z. Accuracy first: Selecting a differential privacy level for accuracy constrained erm. *Advances in Neural Information Processing Systems*, 30, 2017.
- Liu, A., Shen, X., Li, Z., Liu, G., Xu, J., Zhao, L., Zheng, K., and Shang, S. Differential private collaborative web services qos prediction. *World Wide Web*, 22:2697–2720, 2019.
- Liu, X., Kong, W., and Oh, S. Differential privacy and robust statistics in high dimensions. In *Conference on Learning Theory*, pp. 1167–1246. PMLR, 2022.
- Maas, A. L., Daly, R. E., Pham, P. T., Huang, D., Ng, A. Y., and Potts, C. Learning word vectors for sentiment analysis. In *Proceedings of the 49th Annual Meeting of the Association for Computational Linguistics: Human Language Technologies*, pp. 142–150, Portland, Oregon, USA, June 2011. Association for Computational Linguistics. URL <http://www.aclweb.org/anthology/P11-1015>.
- Müller, M. N., Eckert, F., Fischer, M., and Vechev, M. Certified training: Small boxes are all you need. *arXiv preprint arXiv:2210.04871*, 2022.
- Nandi, A. and Bassily, R. Privately answering classification queries in the agnostic pac model. In *Algorithmic Learning Theory*, pp. 687–703. PMLR, 2020.
- Neel, S., Roth, A., and Sharifi-Malvajerdi, S. Descent-to-delete: Gradient-based methods for machine unlearning. In *Algorithmic Learning Theory*, pp. 931–962. PMLR, 2021.
- Nguyen, T. T., Huynh, T. T., Nguyen, P. L., Liew, A. W.-C., Yin, H., and Nguyen, Q. V. H. A survey of machine unlearning. *arXiv preprint arXiv:2209.02299*, 2022.
- Nissim, K., Raskhodnikova, S., and Smith, A. Smooth sensitivity and sampling in private data analysis. In *Proceedings of the thirty-ninth annual ACM symposium on Theory of computing*, pp. 75–84, 2007.
- Papernot, N., Abadi, M., Erlingsson, U., Goodfellow, I., and Talwar, K. Semi-supervised knowledge transfer for deep learning from private training data. *arXiv preprint arXiv:1610.05755*, 2016.
- Radford, A., Wu, J., Child, R., Luan, D., Amodei, D., Sutskever, I., et al. Language models are unsupervised multitask learners. *OpenAI blog*, 1(8):9, 2019.
- Rump, S. M. Fast and parallel interval arithmetic. *BIT Numerical Mathematics*, 39:534–554, 1999.
- Sander, T., Stock, P., and Sablayrolles, A. Tan without a burn: Scaling laws of dp-sgd. In *International Conference on Machine Learning*, pp. 29937–29949. PMLR, 2023.
- Sekhari, A., Acharya, J., Kamath, G., and Suresh, A. T. Remember what you want to forget: Algorithms for machine unlearning. *Advances in Neural Information Processing Systems*, 34:18075–18086, 2021.
- Singh, G., Gehr, T., Püschel, M., and Vechev, M. An abstract domain for certifying neural networks. *Proc. ACM Program. Lang.*, 3(POPL), jan 2019. doi: 10.1145/3290354.
- Song, C., Ristenpart, T., and Shmatikov, V. Machine learning models that remember too much. In *Proceedings of the 2017 ACM SIGSAC Conference on computer and communications security*, pp. 587–601, 2017.
- Sosnin, P. and Tsay, C. Scaling mixed-integer programming for certification of neural network controllers using bounds tightening. *arXiv preprint arXiv:2403.17874*, 2024.
- Sosnin, P., Müller, M., Baader, M., Tsay, C., and Wicker, M. Certified robustness to data poisoning in gradient-based training. *arXiv preprint arXiv:2406.05670*, 2024.
- Tsay, C., Kronqvist, J., Thebelt, A., and Misener, R. Partition-based formulations for mixed-integer optimization of trained relu neural networks. *Advances in neural information processing systems*, 34:3068–3080, 2021.

- van der Maaten, L. and Hannun, A. The trade-offs of private prediction. *arXiv preprint arXiv:2007.05089*, 2020.
- Wicker, M., Huang, X., and Kwiatkowska, M. Feature-guided black-box safety testing of deep neural networks. In *Tools and Algorithms for the Construction and Analysis of Systems: 24th International Conference, TACAS 2018, Held as Part of the European Joint Conferences on Theory and Practice of Software, ETAPS 2018, Thessaloniki, Greece, April 14-20, 2018, Proceedings, Part I 24*, pp. 408–426. Springer, 2018.
- Wicker, M., Laurenti, L., Patane, A., and Kwiatkowska, M. Probabilistic safety for bayesian neural networks. In *Conference on uncertainty in artificial intelligence*, pp. 1198–1207. PMLR, 2020.
- Wicker, M., Heo, J., Costabello, L., and Weller, A. Robust explanation constraints for neural networks. *arXiv preprint arXiv:2212.08507*, 2022.
- Xu, K., Shi, Z., Zhang, H., Wang, Y., Chang, K., Huang, M., Kailkhura, B., Lin, X., and Hsieh, C. Automatic perturbation analysis for scalable certified robustness and beyond. In Larochelle, H., Ranzato, M., Hadsell, R., Balcan, M., and Lin, H. (eds.), *Advances in Neural Information Processing Systems 33: Annual Conference on Neural Information Processing Systems 2020, NeurIPS 2020, December 6-12, 2020, virtual*, 2020. URL <https://proceedings.neurips.cc/paper/2020/hash/0cbc5671ae26f67871cb914d81ef8fc1-Abstract.html>.
- Yang, J., Shi, R., and Ni, B. MedMNIST classification decathlon: A lightweight AutoML benchmark for medical image analysis. In *IEEE 18th International Symposium on Biomedical Imaging (ISBI)*, pp. 191–195, 2021.
- Yu, D., Kamath, G., Kulkarni, J., Liu, T.-Y., Yin, J., and Zhang, H. Individual privacy accounting for differentially private stochastic gradient descent. *arXiv preprint arXiv:2206.02617*, 2022.

## A Related Works

DP has enabled the adoption of privacy-preserving machine learning in a variety of industries (Dwork et al., 2014), yet *post-hoc* audits have revealed a gap between attacker strength and guarantees offered by DP (Carlini et al., 2022; Yu et al., 2022). As a result, several works seek more specific, and thus sharper, privacy guarantees. For example, Nissim et al. (2007) and Liu et al. (2022) use notions of local sensitivity to produce tighter bounds. In Ligett et al. (2017), the authors privately search the space of privacy-preserving parameters to tune performance on a given dataset, while in Yu et al. (2022) the authors propose individual differential privacy, which can compute tighter privacy bounds for given individuals in the dataset. Unlike this work, these rely solely on traditional DP-SGD (Abadi et al., 2016).

On the other hand, DP can additionally provide bounds in the setting of machine unlearning (Sekhari et al., 2021; Huang & Canonne, 2023). In such cases, it is more likely that guarantees are not tight due to the assumption that individuals can be both added and removed, rather than just removed (Huang & Canonne, 2023). The gold standard for unlearning (which incurs no error) is retraining. Yet, keeping the data on hand poses a privacy concern (Dwork et al., 2014), and retraining can be prohibitively costly (Nguyen et al., 2022). If one admits the privacy cost of storing and tracking all data, then retraining costs can be limited (Bourtole et al., 2021). Existing unlearning without retraining are either restricted to linear (Guo et al., 2019) or strongly convex models (Neel et al., 2021).

The privacy setting most similar to the one adopted in this paper is the differential private prediction setting where we are interested in only privatizing the output predictions of a model (Liu et al., 2019). The PATE method may be interpreted in this light (Papernot et al., 2016), but largely this setting has been investigated in the context of learning theory (Bassily et al., 2018; Nandi & Bassily, 2020). In practice, it is found that training-time privacy such as DP-SGD is preferable to prediction-time privacy (van der Maaten & Hannun, 2020). This work can be viewed as proving tighter bounds on the private prediction setting, which allows private prediction to display some benefits over training-time privacy.

The approaches that are computationally similar to the framework established in this paper come from adversarial robustness certification (Katz et al., 2017; Gehr et al., 2018) or robust training (Gowal et al., 2018; Müller et al., 2022). These approaches typically utilize methods from formal methods (Katz et al., 2017; Wicker et al., 2018) or optimization (Huchette et al., 2023; Tsay et al., 2021). Most related to this work are strategies that provide guarantees over varying both model inputs and parameters (Wicker et al., 2020; Xu et al., 2020), as well as work on robust explanations that bound the input gradients of a model (Wicker et al., 2022). Despite some methodological relationships, none of the above methods can apply to the

general training setting without the proposed framework and are unable to make statements about differential privacy.

## B Interval Bound Propagation

In this section, we provide details of the interval bound propagation procedure required to compute the gradient bounds required by Theorem 3.4 in the context of neural network models. We define a neural network model  $f^\theta : \mathbb{R}^{n_0} \rightarrow \mathbb{R}^{n_K}$  with parameters  $\theta := \{(W^{(i)}, b^{(i)})\}_{i=1}^K$  to be a function composed of  $K$  layers:

$$\hat{z}^{(k)} = W^{(k)}z^{(k-1)} + b^{(k)}, \quad z^{(k)} = \sigma(\hat{z}^{(k)})$$

where  $z^{(0)} := x$ ,  $f^\theta(x) := \hat{z}^{(K)}$ , and  $\sigma$  is the activation function, which we take to be ReLU.

The standard back-propagation procedure for computing the gradients of the loss  $\mathcal{L}$  w.r.t. the parameters of the neural network is given by

$$\frac{\partial \mathcal{L}}{\partial z^{(k-1)}} = \left(W^{(k)}\right)^\top \frac{\partial \mathcal{L}}{\partial \hat{z}^{(k)}}, \quad \frac{\partial \mathcal{L}}{\partial \hat{z}^{(k)}} = H(\hat{z}^{(k)}) \circ \frac{\partial \mathcal{L}}{\partial z^{(k)}}$$

$$\frac{\partial \mathcal{L}}{\partial W^{(k)}} = \frac{\partial \mathcal{L}}{\partial \hat{z}^{(k)}} \left(z^{(k-1)}\right)^\top, \quad \frac{\partial \mathcal{L}}{\partial b^{(k)}} = \frac{\partial \mathcal{L}}{\partial \hat{z}^{(k)}}$$

where  $H(\cdot)$  is the Heaviside function, and  $\circ$  is the Hadamard product.

**Interval Arithmetic** Let us denote intervals over matrices as  $\mathbf{A} := [A_L, A_U] \subseteq \mathbb{R}^{n \times m}$  such that for all  $A \in \mathbf{A}$ ,  $A_L \leq A \leq A_U$ . We define the following interval matrix arithmetic operations:

- Addition:  $A + B \in [\mathbf{A} \oplus \mathbf{B}] \forall A \in \mathbf{A}, B \in \mathbf{B}$
- Matrix mul.:  $A \times B \in [\mathbf{A} \otimes \mathbf{B}] \forall A \in \mathbf{A}, B \in \mathbf{B}$
- Elementwise mul.:  $A \circ B \in [\mathbf{A} \odot \mathbf{B}] \forall A \in \mathbf{A}, B \in \mathbf{B}$

Each of these operations can be computed using standard interval arithmetic in at most  $4 \times$  the computational cost of its non-interval counterpart. For example, interval matrix multiplication can be computed efficiently using Rump’s algorithm (Rump, 1999). We denote interval vectors as  $\mathbf{a} := [a_L, a_U]$  with analogous operations.

We will now describe the procedure for propagating intervals through the forward and backward passes of a neural network to compute valid gradient bounds.

**Bounding the Forward Pass** Given these interval operations, for any input  $x \in \mathbf{x}$  and parameters  $W^{(k)} \in \mathbf{W}^{(k)}$ ,  $b^{(k)} \in \mathbf{b}^{(k)}$ ,  $k = 1, \dots, K$ , we can compute intervals

$$\hat{\mathbf{z}}^{(k)} = \mathbf{W}^{(k)} \otimes z^{(k-1)} \oplus \mathbf{b}^{(k)}, \quad \mathbf{z}^{(k)} = \sigma(\hat{\mathbf{z}}^{(k)})$$

such that  $f^\theta(x) \in \hat{\mathbf{z}}^{(K)}$ . The monotonic activation function  $\sigma$  is applied element-wise to both the lower and upper bound of its input interval to obtain a valid output interval. Here we consider only neural networks with ReLU activations, although the interval propagation framework is applicable to many other architectures.

**Bounding the Loss Gradient** Since we are in a classification setting, we will consider a standard cross entropy loss. Given the output logits of the neural network,  $\hat{z}^{(K)} = f^\theta(x)$ , the categorical cross entropy loss function is given by

$$\mathcal{L}(\hat{z}^{(K)}, y) = - \sum_i y_i \log p_i$$

where

$$p_i = \left[ \sum_j \exp(\hat{z}_j^{(K)} - \hat{z}_i^{(K)}) \right]^{-1}$$

is the output of the softmax function and  $y$  is a one-hot encoding of the true label. The gradient of the cross entropy loss  $\mathcal{L}$  with respect to  $\hat{z}^{(K)}$  is given by

$$\frac{\partial \mathcal{L}(\hat{z}^{(K)}, y)}{\partial \hat{z}^{(K)}} = p - y$$

The output of  $p = \text{softmax}(\hat{z}^{(K)})$  given any  $\hat{z}^{(K)} \in [\hat{z}_L^{(K)}, \hat{z}_U^{(K)}]$  is bounded by

$$[p_L]_i = \left[ \sum_j \exp\left(\left[\hat{z}_U^{(K)}\right]_j - \left[\hat{z}_L^{(K)}\right]_i\right) \right]^{-1},$$

$$[p_U]_i = \left[ \sum_j \exp\left(\left[\hat{z}_L^{(K)}\right]_j - \left[\hat{z}_U^{(K)}\right]_i\right) \right]^{-1}.$$

Therefore, an interval over the gradient of the loss  $\mathcal{L}$  with respect to  $\hat{z}^{(K)}$  is given by

$$\frac{\partial \mathcal{L}(\hat{z}, y)}{\partial \hat{z}} = [p_L - y, p_U - y]$$

**Bounding the Backward Pass** Wicker et al. (2022) use interval arithmetic to bound derivatives of the form  $\partial \mathcal{L} / \partial z^{(k)}$  and here we extend this to additionally compute bounds on the derivatives w.r.t. the parameters. Specifically, we can back-propagate  $\partial \mathcal{L} / \partial \hat{z}^{(K)}$  (computed above) to obtain

$$\frac{\partial \mathcal{L}}{\partial z^{(k-1)}} = \left( \mathbf{W}^{(k)} \right)^\top \otimes \frac{\partial \mathcal{L}}{\partial \hat{z}^{(k)}}$$

$$\frac{\partial \mathcal{L}}{\partial \hat{z}^{(k)}} = H\left(\hat{z}^{(k)}\right) \circ \frac{\partial \mathcal{L}}{\partial z^{(k)}}$$

$$\frac{\partial \mathcal{L}}{\partial \mathbf{W}^{(k)}} = \frac{\partial \mathcal{L}}{\partial \hat{z}^{(k)}} \otimes \left( z^{(k-1)} \right)^\top$$

$$\frac{\partial \mathcal{L}}{\partial \mathbf{b}^{(k)}} = \frac{\partial \mathcal{L}}{\partial \hat{z}^{(k)}}$$

where  $H(\cdot)$  applies the Heaviside function to both the lower and upper bounds of the interval, and  $\circ$  is the Hadamard product. The resulting intervals are valid bounds for each partial derivative, that is

$$\frac{\partial \mathcal{L}}{\partial \mathbf{W}^{(k)}} \in \frac{\partial \mathcal{L}}{\partial \mathbf{W}^{(k)}}, \frac{\partial \mathcal{L}}{\partial \mathbf{b}^{(k)}} \in \frac{\partial \mathcal{L}}{\partial \mathbf{b}^{(k)}}$$

for all  $\mathbf{W}^{(k)} \in \mathbf{W}^{(k)}$ ,  $\mathbf{b}^{(k)} \in \mathbf{b}^{(k)}$  and  $k = 1, \dots, K$ .

## C Bounding the Smooth Sensitivity

In this section, we describe in detail the process for computing bounds on the  $\beta$ -smooth sensitivity for a model  $f$  at a point  $x$ , which is given by:

$$S_{\mathcal{D}}^\beta(x) = \max_{k \in \mathbb{N}^+} \Delta_{\mathcal{D}}^k f|_x \exp(-2\beta k) \quad (8)$$

We first note that the AGT provides sound upper bounds  $\Delta_{\mathcal{D}}^k f|_x \leq \text{LS}(\mathcal{T}_k^p, x)$ , and thus the smooth sensitivity is further bounded by

$$S_{\mathcal{D}}^\beta(x) \leq \bar{S}_{\mathcal{D}}^\beta(x) = \max_{k \in \mathbb{N}^+} \text{LS}(\mathcal{T}_k^p, x) \exp(-2\beta k). \quad (9)$$

In this appendix, we only consider the binary classification setting, but the results presented here can additionally be extended to multi-class or (bounded) regression settings (with the appropriate sensitivities multiplied by 2). Therefore, the bounds  $\text{LS}(\mathcal{T}_k^p, x)$  provided by AGT are either 0 (the query at the point  $x$  is certifiably privacy-safe) or 1 (the query at  $x$  is not certified). Additionally,  $\text{LS}(\mathcal{T}_k^p, x)$  is non-decreasing in  $k$ , and so takes the form of a step function

$$\text{LS}(\mathcal{T}_k^p, x) = H(k - k^*(x)) \quad (10)$$

where  $H$  is the Heaviside function and  $k^*(x)$  is the first value of  $k$  at which  $\text{LS}(\mathcal{T}_k^p, x) = 1$ .

Figure 6 shows a plot of the function  $h(k) = \text{LS}(\mathcal{T}_k^p, x) \exp(-2\beta k)$ . While the maximum value  $\bar{S}_{\mathcal{D}}^\beta(x) = \exp(-2\beta k^*)$  is attained at  $k^*$ , it is clear that  $\exp(-2\beta k)$  is a valid upper bound on  $\bar{S}_{\mathcal{D}}^\beta(x)$  for any  $k \leq k^*$ .

Therefore, we employ the following procedure for bounding the smooth sensitivity  $S_{\mathcal{D}}^\beta(x)$ :

1. Choose a set of values  $\mathcal{K} = \{k_i\}_{i=1}^M$  and compute the corresponding parameter-space bounds using Algorithm 1.
2. At a query point  $x$ , find the largest  $k' \in \mathcal{K}$  for which  $\text{LS}(\mathcal{T}_{k'}^p, x) = 0$  (e.g. via binary search).
3. Since  $\text{LS}(\mathcal{T}_{k'}^p, x) = 0$ , we have that  $k' + 1 \leq k^*$  and  $\exp(-2\beta(k' + 1))$  is a sound upper bound on  $S_{\mathcal{D}}^\beta(x)$ .

The set of  $k$  values should be chosen according to the available computational budget. A more fine-grained set of  $k$ 's will achieve tighter sensitivity bounds, as  $k'$  will fall closer to  $k^*$ , on average. On the other hand, increasing the number of  $k$  values increases the computational complexity at both training time (running Algorithm 1 for each  $k$ ) and at inference time (finding  $k'$  via binary search).

In practice, the set  $\mathcal{K}$  should be chosen with greater density for smaller values of  $k$ , as the improvement in the tightness of the bound is more pronounced for lower values of  $k$  due to the exponential decay. Specifically, going from  $k' = 1$  to  $k' = 2$  results in a significantly greater improvement

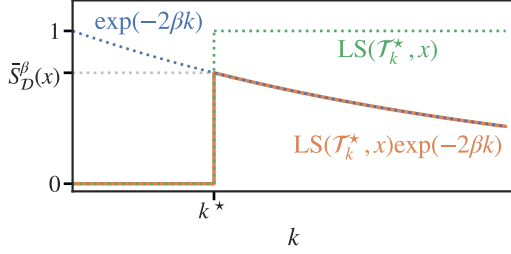


Figure 6: Visualization of the solutions to the smooth sensitivity optimization problem.

than, for example, refining the bound between  $k' = 51$  and  $k' = 52$ .

Furthermore, for sufficiently large values of  $k$ , it is often the case that the resulting bounds do not certify any points within the domain, rendering the inclusion of such large  $k$  values unnecessary. Consequently, it is advantageous to prioritize smaller  $k$  values in the set  $\mathcal{K}$ , where the improvement in the bound is substantial, while avoiding the inclusion of excessively large  $k$  values that offer diminishing returns both in terms of bound improvement and computational efficiency.

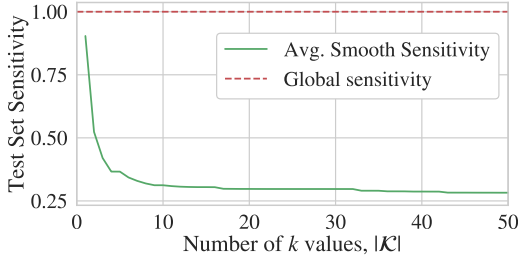


Figure 7: Effect of  $|\mathcal{K}|$  on the tightness of the smooth sensitivity bound for the GTP-2 sentiment classification task ( $\epsilon = 1.0$ ).

Figure 7 illustrates how increasing the number of  $k$  values affects the tightness of our bounds. Even when  $|\mathcal{K}| = 1$  (i.e., AGT is run for a single value of  $k$ ), the smooth sensitivity bound is already tighter than the global sensitivity. As the number of  $k$  values increases, the smooth sensitivity bound becomes progressively tighter. However, after  $|\mathcal{K}| \approx 10$ , the gains diminish, indicating that running AGT for a small number of  $k$  values is sufficient to capture most of the privacy benefits.

## D Proofs

In this section we provide formal proofs of the theorems stated in the main text.

### D.1 Tighter Privacy Accounting (Theorem 3.2)

In this section, we provide a proof of Theorem 3.2. We start by recalling the following from Section 3.1.1:

1. (*Global Sensitivity.*) The algorithm that returns  $f^\theta(x) + \text{Lap}(1/\epsilon)$  is  $(\epsilon, 0)$  differentially private.
2. (*Smooth Sensitivity.*) If  $\beta \leq \epsilon/(2 \ln(2/\delta))$  and  $\delta \in (0, 1)$  the algorithm that returns  $f^\theta(x) + \text{Lap}(2S_{\mathcal{D}}^\beta(x)/\epsilon)$  is  $(\epsilon, \delta)$  differentially private.

Therefore, given a noise level  $\text{Lap}(C)$ , we can calculate the privacy loss under both mechanisms by equating  $C = 1/\epsilon$  or  $C = 2S_{\mathcal{D}}^\beta(x)/\epsilon$ , respectively, and solving for  $\epsilon$ .

We now assume that the noise level is chosen according to the global sensitivity, and aim to solve for the privacy loss under the smooth sensitivity mechanism (which we label  $\epsilon^S$ ):

$$\frac{1}{\epsilon} = \frac{2S_{\mathcal{D}}^\beta(x)}{\epsilon^S}, \quad \epsilon^S = 2S_{\mathcal{D}}^\beta(x)\epsilon \quad (11)$$

Now, setting  $\beta = \epsilon^S/(2 \ln(2/\delta))$ , we have

$$S_{\mathcal{D}}^\beta(x) = \max_{k \in \mathbb{N}^+} \Delta_{\mathcal{D}}^k f|_x \exp(-2\beta k) \quad (12)$$

$$= \exp\left(\frac{-k^* \epsilon^S}{\ln(2/\delta)}\right) \quad (13)$$

for some optimal  $k^*$ . Note that  $k^*$  is independent of the choice of  $\beta$ , and thus does not depend on  $\epsilon^S$ . Substituting into (11) gives

$$\epsilon^S = 2 \exp\left(-2k^* \frac{\epsilon^S}{2 \ln(2/\delta)}\right) \epsilon \quad (14)$$

$$2\epsilon = \epsilon^S \exp\left(\frac{k^* \epsilon^S}{\ln(2/\delta)}\right) \quad (15)$$

and with a change of variables  $\alpha = k^* \epsilon^S / \ln(2/\delta)$  we have

$$\alpha \exp(\alpha) = \frac{2\epsilon k^*}{\ln(2/\delta)} \quad (16)$$

which is solved via the Lambert W (product-log) function

$$\alpha = W\left(\frac{2\epsilon k^*}{\ln(2/\delta)}\right) \quad (17)$$

$$\epsilon^S = \frac{\ln(2/\delta)}{k^*} W\left(\frac{2\epsilon k^*}{\ln(2/\delta)}\right) \quad (18)$$

Since  $2\epsilon k^* / \ln(2/\delta)$  is real and  $> 0$ , this equation always has a solution on the principal branch of  $W$ .  $\square$

### D.2 Algorithm Correctness Proof (Theorem 3.3)

Here we provide a proof of correctness for our algorithm (i.e., proof of Theorem 3.3) as well as a detailed discussion of the operations therein.

First, we recall the definition of valid parameter space bounds (Definition 5 in the main text):

$$\begin{aligned} \theta_i^L &\leq \min_{\mathcal{D}' \in \mathcal{B}_{*,k}(\mathcal{D})} M(f, \theta', \mathcal{D}')_i \\ &\leq M(f, \theta', \mathcal{D})_i \\ &\leq \max_{\mathcal{D}' \in \mathcal{B}_{*,k}(\mathcal{D})} M(f, \theta', \mathcal{D}')_i \leq \theta_i^U \end{aligned}$$

We also recall the iterative equations for stochastic gradient descent:

$$\begin{aligned}\theta^{(0)} &= \theta' \\ \theta^{(i+1)} &= \theta^{(i)} - \alpha \frac{1}{b} \sum_{j=1}^b \nabla_{\theta} \mathcal{L}(f^{\theta^{(i)}}(x^{(j)}), y^{(j)})\end{aligned}$$

For ease of notation, we assume a fixed data ordering (one may always take the element-wise maximums/minimums over the entire dataset rather than each batch to relax this assumption), and we denote  $\theta_{\mathcal{D}}^{(1)}$  as the value of the parameters at the  $i$ -th iteration given the dataset  $\mathcal{D}$  with fixed ordering.

Now, we proceed to prove by induction that Algorithm 1 maintains valid parameter-space bounds for privacy/unlearning at each step of gradient descent. We start with the base case where  $\theta^L = \theta^U = \theta'$  according to line 1, and now we prove that the result of the first batch (lines 7–16) produces a new  $\theta^L$  and  $\theta^U$  that are valid parameter-space bounds (Definition 5). In the first iteration (base case), the definition is trivially satisfied due to the fact that  $\theta^L = \theta^U$ . Lines 7–9 are simply the standard forward and backwards passes, as the optimization is over a singleton set. Subsequently we have update steps for unlearning and privacy respectively:

**Base-case: Privacy Update** To account for the worst-case influence of an arbitrary  $k$  data-points being added to this batch, we note that the clipping step (line 9) limits the largest contribution of these points to  $k\gamma$  and the smallest contribution being  $-k\gamma$ . However, we must account for the case that this batch has  $k$  points added and  $k$  points removed (this is a strict over-approximation that may be improved in future works). In this case, the largest gradient value one can achieve through simultaneous removing and addition is no larger than, for each element, replacing the  $k$  smallest contributions to the average gradient with the value  $k\gamma$ . Correspondingly, the smallest gradient value for simultaneous addition and removal of data points cannot be smaller than replacing, element-wise, the  $k$  largest contributions to the average gradient with  $-k\gamma$ . It is then straightforward to see that the bounds described are captured by the updates on lines 14 and 15, respectively.

**Base-case: Unlearning Update** The unlearning update is effectively a subset of the above privacy case. In this update we must compute the largest and smallest possible gradients one could achieve strictly by removing up to  $k$  points from the batch. In this case, a sound bound on these values is to simply remove the smallest  $k$  contributions to each element of the averaged gradient to upper-bound the gradient change. The corresponding lower-bound is to remove the largest  $k$  contributions to each element of the averaged gradient. This bound is exactly what is expressed in lines 12 and 13.

Provided that one has computed sound bounds described above, denoted  $d^U$  and  $d^L$  respectively, we observe that:

$$\theta' - \alpha d^L \geq \max_{\mathcal{D}' \in \mathcal{B}_{*,k}(\mathcal{D})} \theta_{\mathcal{D}'}^{(1)} \quad (19)$$

$$\theta' - \alpha d^U \leq \min_{\mathcal{D}' \in \mathcal{B}_{*,k}(\mathcal{D})} \theta_{\mathcal{D}'}^{(1)} \quad (20)$$

Finally, by setting  $\theta^U = \theta' - \alpha d^L$  and  $\theta^L = \theta' - \alpha d^U$ , the above inequalities imply that the interval  $[\theta^L, \theta^U]$  satisfies Definition 5, thus proving the base case.

**Inductive hypothesis** Our inductive hypothesis is then that, given that the previous iteration of the algorithm provides valid parameter-space bounds, denoted  $[\theta^L, \theta^U]$ , on the  $i^{\text{th}}$  iteration of SGD for privacy/unlearning, we would like to prove that the algorithm computes valid parameter space bounds on  $\theta^{(i+1)}$ . Unlike our base-case, the optimization problems on lines 7–9 must be computed or at least soundly bounded. For this, we appeal to the soundness of bound propagation techniques through the forward and backwards pass of a neural network, i.e., given in (Wicker et al., 2022). Such bounds allow us to compute the following bounds for any given input-output pair  $(x, y)$ :

$$\delta_L^{(j)} = \min_{\theta^* \in [\theta^L, \theta^U]} \nabla_{\theta^*} \mathcal{L}(f^{\theta^*}(x), y) \quad (21)$$

$$\delta_U^{(j)} = \max_{\theta^* \in [\theta^L, \theta^U]} \nabla_{\theta^*} \mathcal{L}(f^{\theta^*}(x), y) \quad (22)$$

Given these bounds, the update steps from our base cases must be revised. Provided that  $[\theta^L, \theta^U]$  satisfy Definition 5 (true from our assumption starting the inductive hypothesis) we know that the bounds in Equation (21) account for the largest and smallest gradients one can achieve without any data-point additions or removals from the current batch (follows from soundness of bound propagation through the forward and backwards passes). Thus, to capture the largest gradient update one can achieve by simultaneous addition and removal of  $k$  in the current batch, we now follow the same procedure from the base case, but replace the average standard gradients  $\delta$  with the average of the upper-bound on the gradients,  $\delta^U$ . The corresponding change is made to lower-bound the smallest gradient one can achieve. Finally, allowing the bounds  $d^U$  and  $d^L$  to be given by the aggregation described, we again have that:

$$\theta^{(U)} - \alpha d^L \geq \max_{\mathcal{D}' \in \mathcal{B}_{*,k}(\mathcal{D})} \theta_{\mathcal{D}'}^{(i+1)} \quad (23)$$

$$\theta^{(L)} - \alpha d^U \leq \min_{\mathcal{D}' \in \mathcal{B}_{*,k}(\mathcal{D})} \theta_{\mathcal{D}'}^{(i+1)} \quad (24)$$

Given that the above bounds imply that  $[\theta^{(L)} - \alpha d^U, \theta^{(U)} - \alpha d^L]$  are valid parameter space bounds and that the aggregation to achieve these bounds is exactly what is presented in Algorithm 1, we complete our proof that Algorithm 1 returns bounds that satisfy Definition 5, thus proving Theorem 3.3.  $\square$



Dataset	#Samples	#Features	#Epochs	$\alpha$	$\eta$	$b$
AMEX Default Prediction	5531451	188	1	0.001	0.6	-
OCT-MNIST	97477	784	2	0.2	1.0	5000
IMBD Movie Reviews <sup>†</sup>	40000	768	50	0.08	2.0	20000

Table 1: Datasets and Hyperparameter Settings (<sup>†</sup>: Post GPT-2 Embedding)

## E Unlearning

Unlearning concerns itself with removal of a point and has an analogous definition to differential privacy:

**Definition 6.  $\epsilon$ -Approximate Unlearning (Nguyen et al., 2022)** Given the learning algorithm  $M(\cdot)$ , we say the process  $U(\cdot)$  is an  $\epsilon$ -approximate unlearning process if  $\forall S \subset \Theta, \forall x \in \mathcal{D}$ , both of the following hold:

$$\begin{aligned} \mathbb{P}(U(x, \mathcal{D}, M(f, \theta', \mathcal{D})) \in S) &\leq e^\epsilon \mathbb{P}(M(f, \theta', \mathcal{D} \setminus x) \in S) \\ \mathbb{P}(M(f, \theta', \mathcal{D} \setminus x) \in S) &\leq e^\epsilon \mathbb{P}(U(x, \mathcal{D}, M(f, \theta', \mathcal{D})) \in S) \end{aligned}$$

Definition 6 enforces that the result of applying unlearning algorithm  $U$  is probabilistically similar to having trained without the removed sample  $x$  in the first place.

Similarly to the privacy setting, we now define the local (unlearning) sensitivity and unlearning-safe certification. We first denote the set of all datasets with  $k$  or fewer elements removed as  $\mathcal{T}_k^u(\mathcal{D})$ .

**Definition 7. (Local Unlearning Sensitivity)** The local sensitivity of a prediction made by a machine learning model  $f$  trained by  $M$  at a point  $x$ , i.e.,  $y = f^{M(f, \theta', \mathcal{D})}(x)$ , is defined as:

$$\max_{\mathcal{D}' \in \mathcal{T}_k^u(\mathcal{D})} |f^{M(f, \theta', \mathcal{D}')} (x) - f^{M(f, \theta', \mathcal{D})} (x)| \quad (25)$$

We will define the solution to the above problem with the notation  $\Delta_{\mathcal{D}}^{u,k} f|_x$  where  $k$  is the same as in the definition of  $\mathcal{T}_k^u$ .

**Definition 8. (Unlearning-Safety)** A prediction at a point  $x$  made by a machine learning model  $f$  trained by  $M$ , i.e.,  $y = f^{M(f, \theta', \mathcal{D})}(x)$ , is said to be an unlearning-safe prediction if:

$$\Delta_{\mathcal{D}}^{u,k} f|_x = 0 \quad (26)$$

Again, this definition intuitively means that the prediction from the model  $f$  would have been unchanged given up to  $k$  removals from the training data.

**Use Cases for Unlearning-Safe Certificates.** State-of-the-art re-training approaches for unlearning, e.g., SISA (Bourtole et al., 2021), operate by training an ensemble of classifiers on disjoint sets of user data. Upon receiving an unlearning request, the affected model in the ensemble is taken offline to undergo partial retraining. Adversaries may therefore perform a denial-of-service attack by simultaneously submitting  $\mathcal{O}(d \log(d))$  unlearning requests, at which point the entire ensemble may be taken offline for retraining, provided the ensemble comprises  $d$  or fewer models. Given our approach, despite each model receiving up to  $k$  simultaneous unlearning requests, we may

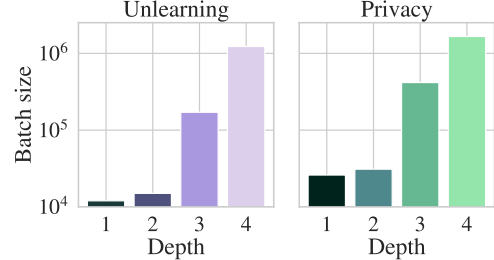


Figure 8: Minimum batch size required to make privacy- or unlearning-safe predictions on at least 95% of the AMEX test data. ( $k = 50$ )

still issue predictions proven to be unlearning-safe, thus increasing the required number of unlearning requests to achieve denial-of-service up to  $\mathcal{O}(kd \cdot \log(kd))$ -many simultaneous requests.

## F Experimental Set-up and Additional Results

### F.1 American Express Default Prediction

In order to understand the performance of our approach in a more practical setting, we turn to the American Express default prediction task. This tabular dataset<sup>5</sup> comprising 5.4 million total entries of real customer data asks models to predict whether a customer will default on their credit card debt. We train networks of varying depth with each layer having 128 hidden nodes. We highlight that fully connected neural networks are generally not competitive in these tasks, thus their accuracy is significantly below competitive entries in the competition. However, this massive real-world dataset in a privacy-critical domain enables us to test the scalability of our approach. In particular, we note that as batch size tends to infinity, our bounds become arbitrarily tight. On the other hand, since we over-approximate the bounds on the gradients using bound-propagation, our bounds weaken super-linearly as the depth of the network increases (Wicker et al., 2020). Figure 8 shows the smallest batch sizes that allow us to train networks of varying depth with privacy and unlearning-safe guarantees for at least 95% of test set inputs. Our approach requires a batch size of over one million to provide these guarantees for 4-layer neural networks. Ignoring the effect of this large batch size on performance for the sake of this particular

<sup>5</sup>See [www.kaggle.com/competitions/amex-default-prediction/](https://www.kaggle.com/competitions/amex-default-prediction/); accessed 05/2024

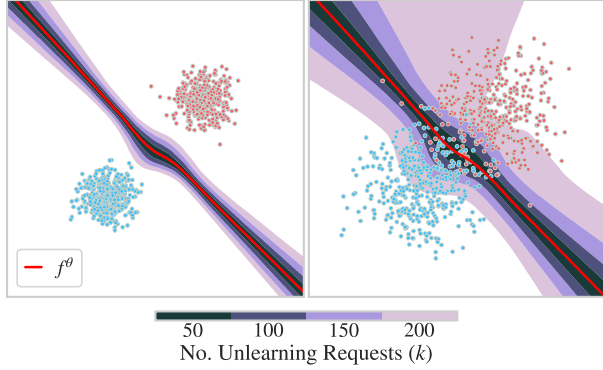


Figure 9: Using the “blobs” dataset, we visualize regions of points enjoying unlearning-safe guarantees for various values of  $k$ . The coloured regions are the regions for which we *cannot* certify predictions for a given  $k$ .

case study, this example highlights that tightly bounding the descent direction (Theorem 3.4), e.g., though bound-tightening approaches (Sosnin & Tsay, 2024), will prove an important line of future research.

## F.2 Unlearning-Safe Certification

**Blobs Dataset.** Mirroring the set-up in Section 4, we present results for the case of unlearning-safe certification in Figure 9. Similar to the privacy case, we observe that strong guarantees of unlearning-safety can be obtained when the data is separable. Where the blobs overlap, however, the effect of removing  $k$  points becomes more pronounced and thus the bounds from AGT become looser. We notice that in both cases, we can provide certificates of unlearning-safety for the majority of the data points for  $k < 150$ .

**MedMNIST Image Classification.** Figure 10 shows the proportion of test-set points with unlearning-safe certificates for the OCT-MNIST fine-tuning task described in Section 4. In comparison to the privacy case, we observe tighter guarantees for unlearning, with values of  $k$  up to 5x larger. Again, we see the corresponding trade-off between certification strength and prediction accuracy when increasing the gradient clipping level  $\gamma$ .

**GPT-2 Sentiment Classification.** We now turn to comparing unlearning and privacy safe certification for the sentiment classification task. Figure 11 shows a comparison of the certificates produced by AGT at each training epoch. In the case of unlearning, AGT can certify a similar proportion of points for values of  $k$  roughly twice as large as in the privacy case. The strength of both unlearning and privacy-safe certification decreases with increasing training time; this may be improved upon in future works via tighter bound-propagation techniques.

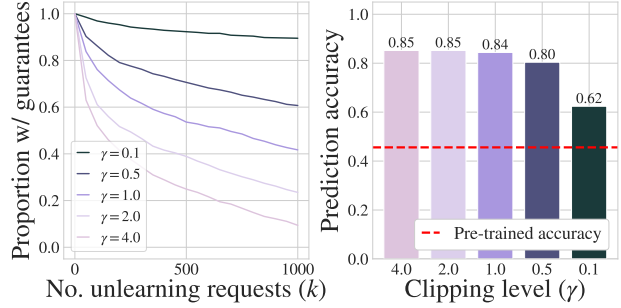


Figure 10: Left: Proportion of the OCT-MNIST test set with unlearning-safe predictions. Right: Prediction Accuracy on the Drusen class.

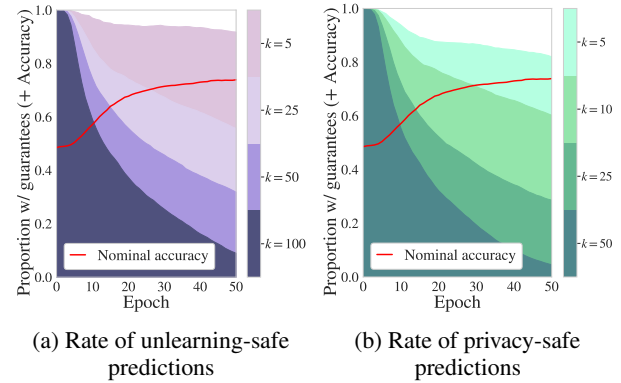


Figure 11: Comparison of unlearning and privacy safe certification using AGT for the GPT-2 sentiment classification task.

## F.3 Experimental Set-up and Hyperparameters

Table 1 provides details of the datasets and hyperparameters used for the experiments in Section 4. For each dataset, we provide the number of epochs, learning rate ( $\alpha$ ), learning rate decay factor ( $\eta$ ) and batchsize ( $b$ ). The decay rate is applied using a standard learning rate schedule  $\alpha_n = \alpha / (1 + \eta n)$ .